THE JOURNAL OF BIOLOGICAL CHEMISTRY
Vol. 280, No. 17, Issue of April 29, pp. 16962–16968, 2005
Printed in U.S.A.

Role for A Kinase-anchoring Proteins (AKAPS) in Glutamate Receptor Trafficking and Long Term Synaptic Depression*

Received for publication, August 23, 2004, and in revised form, February 11, 2005
Published, JBC Papers in Press, February 17, 2005, DOI 10.1074/jbc.M409693200

Eric M. Snyder‡§, Marcie Colledge¶§‖, Robert A. Crozier‡, Wendy S. Chen‡, John D. Scott¶, and Mark F. Bear‡**

From the ‡Howard Hughes Medical Institute, The Picower Center for Learning and Memory and Department of Brain and Cognitive Sciences, Massachusetts Institute of Technology, Cambridge, Massachusetts 02139 and ¶Howard Hughes Medical Institute, Vollum Institute, Oregon Health and Science University, Portland, Oregon 97239

Expression of *N*-methyl D-aspartate (NMDA) receptor-dependent homosynaptic long term depression at synapses in the hippocampus and neocortex requires the persistent dephosphorylation of postsynaptic protein kinase A substrates. An attractive mechanism for expression of long term depression is the loss of surface AMPA (α-amino-3-hydroxy-5-methylisoxazale-4-propionate) receptors at synapses. Here we show that a threshold level of NMDA receptor activation must be exceeded to trigger a stable loss of AMPA receptors from the surface of cultured hippocampal neurons. NMDA also causes displacement of protein kinase A from the synapse, and inhibiting protein kinase A (PKA) activity mimics the NMDA-induced loss of surface AMPA receptors. PKA is targeted to the synapse by an interaction with the A kinase-anchoring protein, AKAP79/150. Disruption of the PKA-AKAP interaction is sufficient to cause a long-lasting reduction in synaptic AMPA receptors in cultured neurons. In addition, we demonstrate in hippocampal slices that displacement of PKA from AKADs occludes synaptically induced long term depression. These data indicate that synaptic anchoring of PKA through association with AKAPs plays an important role in the regulation of AMPA receptor surface expression and synaptic plasticity.

Hippocampal long term synaptic depression (LTD)[1] is induced by appropriate activation of postsynaptic NMDA receptors (1) and is expressed by a reduction in AMPA receptor-mediated currents (2). Dephosphorylation of postsynaptic protein kinase A (PKA) substrates appears to be both necessary and sufficient for expression of LTD in area CA1 of the hippocampus. For example, postsynaptic inhibition of PKA depresses synaptic transmission and occludes LTD (3) and reversal of LTD with high frequency synaptic stimulation (depression) is selectively blocked by PKA inhibitors (4). In addition, LTD correlates with the persistent (>1 h) dephosphorylation of a PKA site on AMPA receptors, Ser^{845} of the GluR1 subunit (4, 5). Dephosphorylation of Ser^{845} decreases AMPA receptor-mediated currents (6, 7) and is therefore likely to contribute directly to LTD expression.

It is now clear that another consequence of NMDA receptor activation is clathrin-mediated endocytosis of AMPA receptors (8–11). Although these data strongly suggest that AMPA receptor internalization also contributes to the expression of LTD, several questions remain. First, it is surprising to note that NMDA receptor activation has not yet been shown to cause a stable long term reduction in surface-expressed AMPA receptors. In fact, the work from Ehlers (10) shows that NMDA receptor activation causes only a transient internalization of AMPA receptors (10). For LTD to be expressed by a reduction in the number of AMPA receptors, it must be possible for NMDA receptor activation to trigger a persistent change. Second, it is not clear what role dephosphorylation of PKA substrates plays in this process. Several findings suggest that the state of phosphorylation of Ser^{845} of GluR1 may regulate its surface expression. Recent work shows that PKA phosphorylation of GluR1 at Ser^{845} is necessary for synaptic delivery of AMPA receptors (12), whereas AMPA receptors internalized in response to NMDA have been shown to be dephosphorylated at GluR1 Ser^{845} (10). In addition, transgenic mice with targeted serine to alanine mutations at Ser^{845} and Ser^{831} of GluR1 are deficient in AMPA receptor endocytosis (13). However, it remains to be determined whether dephosphorylation of PKA substrates is sufficient for decreased AMPA receptor surface expression (as it is for LTD), and if so, what mechanisms account for such dephosphorylation. One of the goals of the current study was to address these questions.

Specificity in PKA signaling arises in part from the association of the enzyme with A kinase-anchoring proteins (AKAPs), which function to target PKA to specific substrates at precise subcellular locations (14, 15). At the postsynaptic density, PKA is tethered to the neuronal anchoring protein, AKAP79/150 (human/rodent) (16, 17). Through association with the synaptic scaffolding MAGUK (membrane-associated guanylate kinase) proteins, AKAP79/150 and its associated enzymes (PKA, protein kinase C, and PP2B) are directed to both NMDA- and AMPA-type glutamate receptors (17). Furthermore, AKAP79/150 has been shown to regulate AMPA receptor phosphorylation and function (17–20). Recent experiments have shown that the synaptic localization of AKAP79/150 itself can be altered by NMDA receptor activation and PP2B signaling cascades, suggesting that AKAP79/150 may play an important role in synaptic plasticity (21). Another aim of this study was to test whether PKA-AKAP interactions are important in regulating AMPA re-

* This work was supported in part by National Institutes of Health Grants GM48231 (to J. D. S.) and NS39321 (to M. F. B.). The costs of publication of this article were defrayed in part by the payment of page charges. This article must therefore be hereby marked "*advertisement*" in accordance with 18 U.S.C. Section 1734 solely to indicate this fact.

§ Both authors contributed equally to work.

‖ Present address: Dept. of Psychiatry, University of Texas Southwestern Medical Center, Dallas, TX 75390.

** To whom correspondence should be addressed: MIT, E19–551, 77 Massachusetts Ave., Cambridge, MA 02139. Tel.: 617-324-7002; Fax: 617-324-7007; E-mail: mbear@mit.edu.

[1] The abbreviations used are: LTD, long term synaptic depression; PKA, cyclic AMP-dependent protein kinase A; AKAP, A kinase-anchoring protein; EPSC, excitatory postsynaptic current; NMDA, *N*-methyl D-aspartate; AMPA, α-amino-3-hydroxy-5-methylisoxazole-4-propionate; PP2B, protein phosphatase 2B.

ceptor surface expression, synaptic transmission, and LTD.

Here we show that an NMDA treatment known to cause LTD in hippocampal slices ("chemLTD") causes a long term reduction in surface AMPA receptor expression in cultured hippocampal neurons. Interestingly, the chemLTD treatment also causes displacement of PKA from the synaptic compartment. We find that inhibiting PKA or disrupting anchoring of PKA to AKAPs is sufficient to reduce surface expression of AMPA receptors. Finally, we demonstrate that the disruption of PKA-AKAP interactions in hippocampal slices leads to a depression of synaptic transmission that occludes synaptically evoked LTD. These data demonstrate a critical role for PKA and AKAPs in the regulation of surface expression of AMPA receptors and LTD.

MATERIALS AND METHODS

Dissociated Hippocampal Cell Culture—All of the rats were housed either in the Brown University Animal Care Facility or Vollum Institute Animal Care Facility, and all of the procedures were approved by institutional animal care and use committees. The hippocampus was removed from P0-P2 Long-Evans rats, exposed to papain (20 units/ml) at 37 °C for 60 min, and dissociated by trituration. Cells were plated onto polylysine-coated (1 mg/ml) dishes. For immunocytochemistry, cells were plated at 75,000 cells/ml (1.5 ml/dish). For biochemistry, cells were plated at 500,000 cells/ml. Cultures were grown in Dulbecco's modified Eagle's medium with 5% fetal bovine serum, 4 mM L-glutamine, B-27 nutrient supplement, and penicillin-streptomycin.

Immunocytochemistry—Following experimental treatment, low density cultures were fixed in 4% paraformaldehyde with 4% sucrose for 5 min. Cultures were then rinsed 2 × 15 min in phosphate-buffered saline and blocked and permeabilized in phosphate-buffered saline containing 20% fetal bovine serum and 0.25% Triton X-100 for 60 min. Cultures were labeled with antibodies against synapsin 1 (1:1000, Chemicon AB1543), synaptophysin (1:500, Chemicon MAB368), GluR2 (1:300 MAB397, Chemicon), and GluR1 (1:300, Upstate Biotechnology, 06-306) overnight at 4 °C. Cultures were then washed 2 × 20 min and exposed to the appropriate fluorescent secondary antibodies (1:300, Jackson Immunoresearch) for 1 h at room temperature. Cultures were washed 2 × 20 min and coverslipped in Vectashield (Vector Laboratories).

Image Analysis—All of the analysis was performed blind to history of the culture. Cultures were visualized using a Olympus Fluo-view Confocal microscope equipped with a ×60 objective. Images were analyzed in NIH Image 1.63. Puncta were defined as regions of staining with greater than 2-fold intensity relative to background staining on neurons. Synaptic GluR2 or GluR1 puncta were defined as puncta with overlapping synaptophysin or synapsin 1 staining.

Biochemical Measurements of Surface Receptor Levels—Detailed methods for biotinylation experiments were described previously (22). Following treatment, 7–14-day-old high density cultured hippocampal neurons were placed on ice to inhibit receptor trafficking and washed twice with ice-cold artificial cerebrospinal fluid (in mM): 124 NaCl; 5 KCl; 1.25 NaH_2PO_4; 26 $NaHCO_3$; 0.8 $MgCl_2$; 1.8 $CaCl_2$; and 10 dextrose saturated with 95% O_2, 5% CO_2. Cultures were then incubated with artificial cerebrospinal fluid containing 1 mg/ml Sulfo-NHS-LC-biotin (sulfosuccinimidyl-6-(biotinamide)hexanoate) (Pierce) for 30 min on ice. Cultures were rinsed in Tris-buffered saline to quench the biotin reaction. Cultures were lysed in 300 μl of modified radioimmune precipitation assay buffer (1% Triton X-100, 0.1% SDS, 0.5% deoxycholic acid, 50 mM $NaPO_4$, 150 mM NaCl, 2 mM EDTA, 50 mM NaF, 10 mM sodium pyrophosphate, 1 mM sodium orthovanadate, 1 mM phenylmethylsulfonyl fluoride, and 1 mg/ml leupeptin). The homogenates were centrifuged at 14,000 × *g* for 15 min at 4 °C. The supernatant (200 μl) was incubated with 100 μl of 50% NeutrAvidin-agarose (Pierce) for 3 h or overnight at 4 °C. NeutrAvidin-bound proteins were washed three times with radioimmune precipitation assay buffer and resuspended in 40 μl of SDS sample buffer and boiled. Quantitative Western blots were performed on biotinylated (surface) proteins using anti-GluR1 C-terminal antibodies (1:1000; Upstate Biotechnology) and transferrin receptor antibodies (1:1000; monoclonal clone H68.4 Zymed Laboratories Inc. Immunoreactive bands were visualized by ECL (Amersham Biosciences or Pierce), captured on autoradiography film (Amersham Biosciences Hyperfilm ECL or Kodak Biomax film). Digital images produced by densitometric scans of autoradiographs on a ScanJet IIcx (Hewlett Packard, Palo Alto, CA) with DeskScan II software (Hewlett Packard) were quantified using NIH Image 1.61 or 1.63 software. Previous control experiments confirmed that the intracellular protein actin was not biotinylated in this assay ($n = 3$). Care was always taken to work within the linear range of this assay.

Synaptosomal Membrane Preparation—Homogenate and P3 synaptosomal membrane fractions were prepared from cortical neuron cultures to increase the yield of protein (10). Occipital cortices of P0-P2 Long-Evans rat pups were rapidly dissected in ice-cold Neurobasal A media (Invitrogen) containing 3 mM $MgCl_2$ and 1 mg/ml kynurenic acid to prevent excitotoxicity. Neurons were plated at high density (530 cells/mm^2) in polylysine-coated dishes. Cells were fractionated at 16–20 days *in vitro*. Neurons were pelleted and homogenized in HEPES-buffered sucrose (4 mM HEPES, pH 7.4, 0.32 M sucrose, 1:100 phosphatase inhibitor cocktails I & II, and 1:100 protease inhibitor mixture III (Calbiochem)) in a glass-glass homogenizer using 50 even strokes and then centrifuged at 1000 × *g* for 10 min to remove nuclei and large debris (P1). The supernatant was then centrifuged at 10,000 × *g* for 15 min to pellet the synaptosome fraction (P2). The P2 pellet was washed in HEPES-buffered sucrose and centrifuged again at 10,000 × *g* for 15 min to pellet the washed synaptosome fraction (P2′). P2′ pellets were lysed in 4 mM HEPES, pH 7.4, and then centrifuged at 25,000 × *g* for 20 min to pellet the synaptosomal membrane fraction (P3). Homogenate and P3 fractions were solubilized in 1% SDS, the protein concentration was determined, and the samples were analyzed by immunoblotting.

Electrophysiology—Long-Evans rats aged P14-P20 (Charles River) were deeply anesthetized with an injection of Beuthanasia-D. Following the disappearance of corneal reflexes and a tail pinch response, the rat was decapitated according to U. S. Department of Health and Human Services and Brown University animal care guidelines. The brain was rapidly removed and placed into ice-cold dissection buffer consisting of the following: 212 mM sucrose; 10 mM glucose; 2.6 mM KCl; 1.23 mM NaH_2PO_4; 26 mM $NaHCO_3$; 9 mM $MgCl_2$; and 1 mM $CaCl_2$. Slices of hippocampus (350 μm) were prepared using a vibrating microtome, and connections from CA3 and subiculum were severed to prevent epileptiform activity. Slices were transferred to a chamber containing artificial cerebrospinal fluid that consisted of the following: 124 mM NaCl; 2.5 mM KCl; 1.23 mM NaH_2PO_4; 26 mM $NaHCO_3$; 1 mM $MgCl_2$; 2.2 mM $CaCl_2$; and 10 mM dextrose. Slices were allowed to recover at room temperature for a minimum of 1 h prior to recording.

For recordings, a slice was transferred to a submersion-type recording chamber and perfused with room temperature (25 °C) or warmed (30 °C) oxygenated artificial cerebrospinal fluid that also contained 50 μM picrotoxin to inhibit γ-aminobutyric acid, type A responses. Temperature differences did not affect results, so the data from the two temperatures were pooled. Individual CA1 pyramidal neurons were visualized using an inverted microscope (Nikon) outfitted with a ×40 and 0.8 numerical aperture objective and IR-DIC optics. Whole-cell voltage-clamp recordings were performed using patch pipettes made of thick walled glass (Sutter, 1.5 mm outer density and 0.86 mm inner density) and filled with internal solution containing the following: 107 mM D-gluconic acid; 107 mM CsOH; 5 mM QX-314 chloride; 0.2 mM EGTA; 20 mM HEPES; 3.7 mM NaCl; 4 mM Mg-ATP; 0.3 mM sodium-GTP; and 10 mM phosphocreatine, pH 7.2. Pipette resistances were 3–5 (Fig. 7*A*) or 7–10 megohms for recordings that required a smaller tip diameter (Fig. 7*B*). Experiments were performed using a patch clamp amplifier (Axopatch 200B), and data were acquired and analyzed using a system from DataWave Technologies (Boulder, CO). Experiments were included in the data set if the base-line period was stable, series resistance was stable (<±20%) for the duration of a recording, and monosynaptic EPSCs were evoked. Experiments were also rejected if Rs > 35 megohms. EPSCs were elicited by delivering a 100-μs current pulse with a 2-contact cluster electrode (FHC, 2 × 25-μm Pt/Ir) placed in stratum radiatum. Test stimuli were delivered at 0.05 Hz, and stimulation intensity was titrated to elicit reliably a monosynaptic EPSC with few failures. The test potential for all of the recordings was −70 mV. LTD was induced by pairing a 1-Hz stimulation with membrane depolarization to −40 mV for 5 min (23). EPSCs were analyzed by measuring the peak amplitude of the response. For statistical comparisons of LTD, data were normalized to the average of a base-line period at 15 min prior to the onset of the pairing protocol and then compared with responses 25–30 min following the completion of the pairing protocol. Data are expressed as mean ± S.E. Stearated Ht31 and Ht31p were used at 1 μM and were interleaved with no peptide controls. Ht31 and Ht31p were purchased from Promega. All of the other reagents were from Sigma.

Statistical Analysis—Statistics were computed using Prism 3.0. Unless otherwise noted, statistical differences were detected by one-way analysis of variance with Bonferroni comparisons between groups.

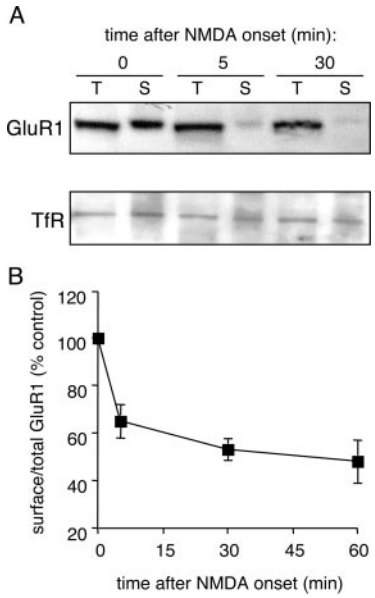

FIG. 1. **ChemLTD NMDA treatment causes a rapid and long-lasting decrease in surface GluR1.** *A*, cultured hippocampal neurons were treated with NMDA (20 μM, 3 min), and surface receptors were biotinylated 5, 30, or 60 min later. NMDA causes a rapid loss of surface (*S*) GluR1 but no change in total (*T*) receptor levels. Levels of the transferrin receptor (*TfR*) were not affected. *B*, NMDA reduced surface/total GluR1 ratio to 63 ± 7% control levels within 5 min ($n = 5$), to 53 ± 6% at 30 min ($n = 5$), and to 48 ± 6% by 60 min ($n = 12$).

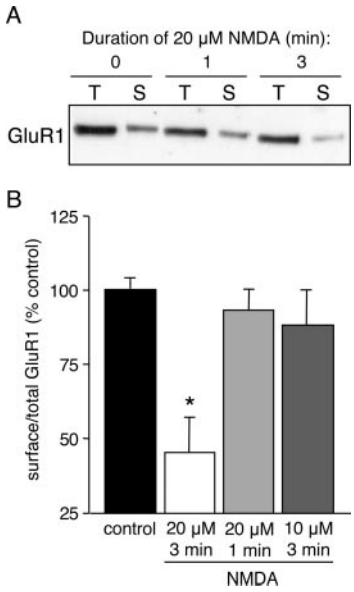

FIG. 2. **A high threshold of NMDA receptor activation is required to induce a long term reduction in surface GluR1.** *A*, total (*T*) and surface (*S*) GluR1 levels were measured 60 min following NMDA (20 μM). A 1-min NMDA treatment induces little or no change, whereas a 3-min treatment greatly reduces surface GluR1. *B*, surface GluR1 was decreased 60 min following the chemLTD NMDA treatment (20 μM, 3 min; 45 ± 11% controls; $n = 4$; *, $p < 0.04$ *versus* control, Student's *t* test). In contrast, GluR1 levels were unaffected following a more brief (20 μM, 1 min) NMDA treatment (92 ± 8% controls; $n = 4$) or treatment with lower concentration of NMDA (10 μM, 3 min; 88 ± 11% control; $n = 4$).

RESULTS

Previous experiments have shown that brief application of NMDA (20 μM, 3 min) initiates LTD in hippocampal slices that persists for at least 1 h (5). Using a biotinylation assay, we tested whether this protocol could cause a long term reduction in surface levels of AMPA receptors in cultured hippocampal neurons. Following NMDA treatment (20 μM, 3 min), cultures were incubated at 37 °C for various times (5, 30, or 60 min) to allow for receptor trafficking. Trafficking was halted by placing cells on ice, and the surface receptors were labeled with biotin (22, 24). Cell extracts were prepared, and biotinylated surface proteins were isolated by NeutrAvidin precipitation. Western blots of surface GluR1 showed that NMDA application caused a rapid reduction in surface AMPA receptors, which was stable for at least 60 min (Fig. 1, *A*, *top panel*, *S*, and *B*). Total cellular levels of GluR1 were unchanged (Fig. 1*A*, *top panel*, *T*). NMDA did not affect the surface levels of the transferrin receptor, a protein known to be continually recycled, demonstrating a relatively specific action on AMPA receptors (Fig. 1*A*, *lower panel*, *TfR*). Surface GluR1 levels were reduced to 48 ± 6% control levels (untreated) 60 min following NMDA treatment (Fig. 1*B*; $p < 0.01$; $n = 12$). We found qualitatively similar results with cortical neuron cultures (surface GluR1 levels were reduced to 57 ± 4% control levels; $n = 5$).

It has been reported that a very similar NMDA treatment (20 μM, 1–2 min) causes only a transient internalization of AMPA receptors in cultured cortical neurons, lasting <30 min. Therefore, we wondered whether a threshold level of NMDA receptor activation must be exceeded to induce a stable loss of surface receptors. Consistent with this notion, we found that shortening the duration of NMDA treatment from 3 to 1 min (Fig. 2, *A* and *B*) or decreasing the concentration of NMDA from 20 to 10 μM failed to induce a significant loss of surface AMPA receptors measured at 60 min (Fig. 2*B*). This dose dependence is reminiscent of previous findings that chemLTD in hippocampal slices could not be induced by lower NMDA concentrations (5).

LTD can be blocked by the application of adenylyl cyclase activators, such as forskolin, or the cell-soluble cAMP analogue, Sp-cAMPS (3). LTD is also reversed by introducing these compounds postsynaptically, indicating that sustained dephosphorylation of postsynaptic PKA substrates is necessary for LTD expression. If NMDA-induced reduction of surface AMPA receptors similarly requires persistent dephosphorylation of PKA substrates, the effects of NMDA on surface expression should be reversed by activating PKA. To test this hypothesis, we treated cultures with NMDA (20 μM, 3 min), waited 30 min to allow for the net loss of surface AMPA receptors, and then treated the cultures with forskolin (Fig. 3*A*, *forsk*; 50 μM, 30 min). Following this treatment protocol, cultures were immediately biotinylated and surface GluR1 levels were quantified. As shown in Fig. 3, chasing NMDA with forskolin restored surface AMPA receptor expression nearly to control levels (Fig. 3, *B* and *C*; 83 ± 8% control; $n = 8$) compared with NMDA treatment alone (48 ± 7% control). However, NMDA + forskolin still causes a significant loss of surface AMPA receptors compared with forskolin alone (reduced to 76 ± 5% forskolin alone control; $p < 0.04$). This percent reduction is less than but not significantly different from what is observed with NMDA alone.

Since postsynaptic inhibition of PKA has been shown to depress synaptic transmission and occlude LTD (3), we next examined whether inhibiting PKA activity might be sufficient to reduce expression of surface AMPA receptors. We treated cultures with Rp-cAMPS (100 μM), an analogue of cAMP that inhibits PKA, and found a significant reduction in surface GluR1 levels to 82 ± 6% controls ($p < 0.05$, $n = 6$, Fig. 3, *D* and *E*). These data are consistent with the idea that persistent dephosphorylation of PKA substrates causes a stable reduction in AMPA receptor surface expression.

We hypothesized that displacement of PKA from the synapse might be one mechanism to account for such persistent dephosphorylation. To test this theory, we subjected cultured cortical

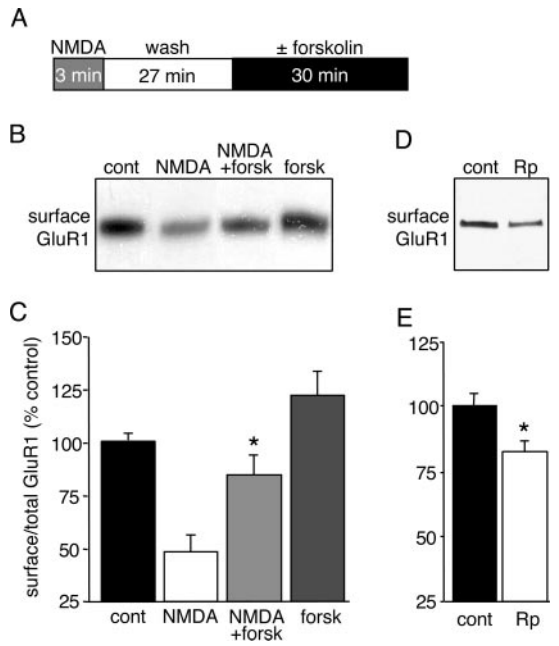

FIG. 3. **PKA regulates surface AMPA receptor levels.** *A*, schematic of the experimental protocol. Cultures were treated with NMDA for 3 min, returned to the incubator for 27 min, and then treated with forskolin (*forsk*) to activate PKA. *B*, representative immunoblot for surface GluR1 showing that forskolin reverses the NMDA-induced loss of surface GluR1. *C*, NMDA reduces surface GluR1 to 48 ± 7% controls. Forskolin significantly reverses this effect (83 ± 8%; $n = 8$; *, $p < 0.05$ *versus* NMDA alone, Student's *t* test). *D*, blocking PKA activity with Rp-cAMPS (*Rp*) causes a reduction in surface GluR1. *E*, Rp-cAMPs significantly reduces surface GluR1 to 82 ± 6% control levels. ($n = 6$; *, $p < 0.05$ *versus* control, Student's *t* test).

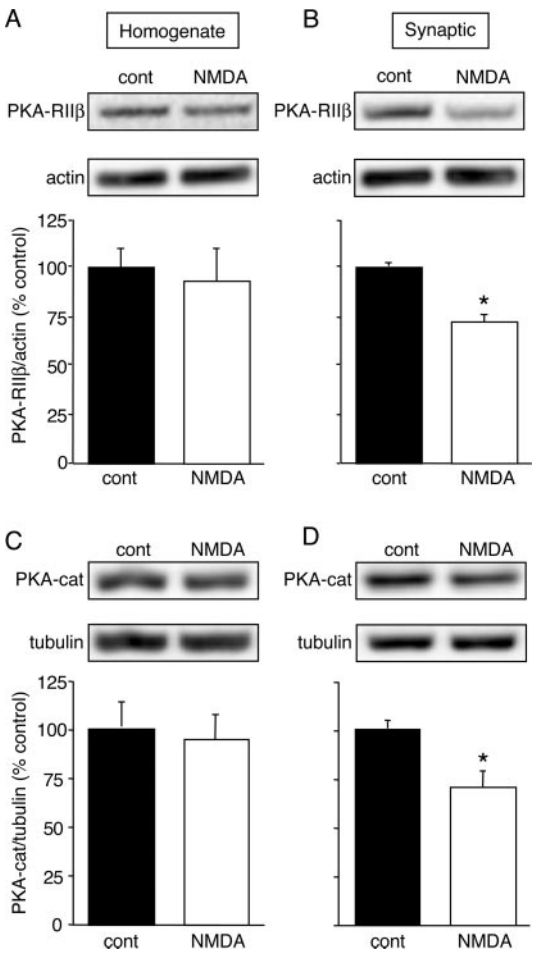

FIG. 4. **ChemLTD NMDA treatment causes displacement of PKA from synaptosomal membrane fractions.** *A*, NMDA treatment causes no change in total levels of PKA regulatory subunit IIβ (*PKA-RIIβ*) in neuronal homogenates (93 ± 18% control, *cont*). *B*, in contrast, NMDA causes a significant reduction in levels of PKA-RIIβ in synaptic (P3) fractions (72 ± 5% control; *, $p < 0.01$ *versus* control, Student's *t* test). *C*, similarly, NMDA treatment causes no change in levels of catalytic subunit of PKA (*PKA-cat*) in total homogenates (94 ± 14% control). *D*, in synaptic fractions, however, NMDA reduces PKA-cat to 71 ± 9% control levels (*, $p < 0.05$ *versus* control (*cont*), Student's *t* test).

neurons to the chemLTD treatment, biochemically fractionated the extracts to isolate total homogenate and synaptosomal membrane fractions, and assessed the fractions for changes in the levels of PKA (Fig. 4). In total homogenates, NMDA caused no change in the levels of the PKA regulatory subunit (Fig. 4*A*, *PKA-RIIβ*; control 100 ± 11%; NMDA 93 ± 18%; $p > 0.7$; $n = 8$) or catalytic subunit (Fig. 4*C*, *PKA-cat*, control 100 ± 13%; NMDA 94 ± 14%; $p = 0.7$; $n = 6$). However, in synaptic fractions, NMDA treatment caused significant reductions in both PKA regulatory subunit IIβ (Fig. 4*B*) and catalytic subunit of PKA (Fig. 4*D*). Following NMDA treatment, synaptic PKA regulatory subunit IIβ levels were reduced to 72 ± 5% control levels (Fig. 4*B*; control 100 ± 3%; $p < 0.01$; $n = 10$). Similarly, synaptic PKA catalytic subunit levels were reduced to 71 ± 9% control levels (Fig. 4*D*; control 100 ± 5%; $p < 0.01$; $n = 7$). These data indicate that the chemLTD NMDA treatment causes a displacement of the PKA holoenzyme from synaptic sites, providing a potential mechanism for maintained dephosphorylation of its substrates.

Specificity in PKA signaling is achieved in part through AKAPs, which target PKA to its appropriate substrates (14). AKAP79/150 previously has been shown to facilitate phosphorylation of Ser^{845} of GluR1 and regulate AMPA-mediated currents (17, 19). Therefore, we wondered whether disruption of PKA anchoring to AKAPs would mimic the chemLTD effect on surface AMPA receptor expression. To test this possibility, we treated cultures with the anchoring inhibitor peptide Ht31 (Fig. 5). Ht31 corresponds to the PKA-binding site of a human thyroid AKAP and competes for binding of PKA to AKAPs, essentially acting as a competitive antagonist of PKA anchoring (16). It should be noted that Ht31 acts only to displace PKA from its anchored sites and has no effect on PKA activity. When stearated (as in these experiments), the peptide is membrane-permeable (25). Treatment of cultured hippocampal neurons with Ht31 (50 μM, 60 min) caused a significant reduction in surface GluR1 (Fig. 5, *A* and *B*; 65 ± 5% control, $p < 0.03$, $n = 8$). In contrast, the control peptide, Ht31p (in which two proline residues replace residues important for binding to PKA and thus prevent competition for PKA anchoring) had no effect on surface levels of GluR1 (Fig. 5, *A* and *B*; 50 μM, 60 min, 96 ± 4% control, $p = 0.3$, $n = 4$). These data indicate that disruption of anchoring of PKA to its synaptic substrates via AKAPs promotes a loss of surface AMPA receptors.

AKAP79/150 anchors both PKA and PP2B in proximity to the AMPA receptor (17, 20, 26, 27). Ht31 causes a rundown of AMPA receptor currents in hippocampal neurons, presumably by favoring activation of anchored PP2B (7, 18, 19). To determine whether this Ht31-induced reduction in surface AMPA receptor levels requires the action of PP2B, we pretreated cultures with ascomycin (an analogue of FK506; 2 μM, 60 min), a specific inhibitor of PP2B (28–30), prior to treatment with Ht31 (50 μM, 60 min). Ascomycin alone had no significant effect on AMPA receptor surface expression (Fig. 5, *C* and *D*; 108 ± 4% Me_2SO vehicle; $p > 0.4$; $n = 3$); however, ascomycin did block the Ht31-induced loss of surface AMPA receptors (Fig. 5, *C* and *D*; 102 ± 10% control, $p > 0.2$, $n = 3$). These observations

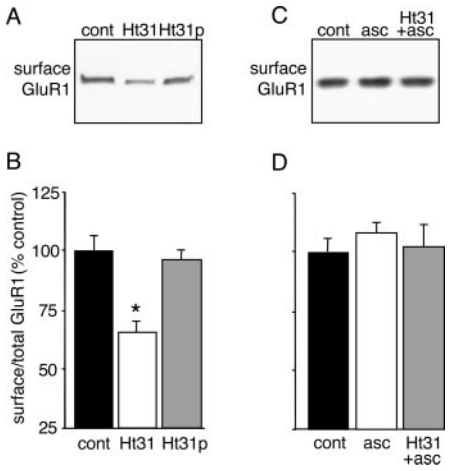

FIG. 5. **Disruption of PKA anchoring to AKAPs is sufficient to cause a reduction in surface GluR1.** *A*, representative immunoblots demonstrating that disrupting PKA-AKAP binding with stearated Ht31 peptide decreases surface GluR1. Control (*cont*) peptide Ht31p has no effect on surface GluR1. *B*, quantification revealed that Ht31 (50 μM, 60 min) reduces surface GluR1 to 65 ± 5% control levels ($n = 8$; *, $p < 0.03$ *versus* control, Student's *t* test). Ht31p has no effect (96 ± 4%; $n = 4$). *C*, the effect of Ht31 on AMPA receptor surface expression is blocked by the PP2B inhibitor ascomycin (*asc*; 2 μM, 60 min). *D*, ascomycin alone has no effect on surface GluR1 levels (108 ± 4% control; $n = 3$) but blocks the Ht31-induced loss of surface GluR1 (102 ± 10%, $n = 3$).

are consistent with the hypothesis that Ht31 displaces PKA from AKAPs, thereby favoring PP2B activity. In the absence of anchored PKA activity, basal PP2B activity is apparently sufficient to reduce surface expression of AMPA receptors.

A possible consequence of attenuated AMPA receptor surface expression is an increase in the proportion of synapses lacking AMPA receptors (8, 9, 31–33). To determine whether AKAP-anchored PKA is important for regulating synaptic AMPA receptors, we treated cultures with Ht31 or control Ht31p and then labeled cultures for the AMPA receptors subunits (Fig. 6). In untreated cultures, 74 ± 8% GluR2 puncta colocalized with synapsin 1 staining (Fig. 6*E*; $n = 7$ cells, 150 synapses) and 64 ± 10% GluR1 puncta colocalized with synaptophysin staining (Fig. 6*J*; $n = 7$ cells, 150 synapses). Ht31 treatment dramatically reduced both synaptic GluR2 and GluR1 staining (Fig. 6, *D* and *I*). 1 h following Ht31 application, only 28 ± 6% synapses contained GluR2 (Fig. 6*E*; $n = 7$ cells, 150 synapses; $p < 0.01$). Similarly, Ht31 reduced synaptic GluR1 staining to 15 ± 9% synapses (Fig. 6*J*; $n = 7$ cells, 150 synapses; $p < 0.01$). In contrast, cultures treated with Ht31p were indistinguishable from controls, expressing GluR2 at 70 ± 6% synapses (Fig. 6, *A*, *B*, and *E*) and GluR1 at 60 ± 10% synapses (Fig. 6, *F*, *G*, and *J*). These data indicate that disruption of PKA anchoring to AKAPs is sufficient to cause a reduction in synaptic AMPA receptors.

Previous electrophysiological studies demonstrated that disruption of the PKA-AKAP association by Ht31 causes a rundown of AMPA receptor-mediated transmission in cultured neurons (18, 19). As with LTD, Ht31-induced rundown is calcium- and PP2B-dependent (19). We hypothesized that disruption of the PKA-AKAP interaction would also block synaptically evoked LTD in hippocampal slices. To test this possibility, we performed whole-cell voltage-clamp recordings of CA1 pyramidal cells and used a pairing protocol to induce LTD (Fig. 7) (23). LTD was reliably induced under two control conditions: 1) either in the absence of any peptide or 2) in the presence of intracellularly introduced Ht31p (Fig. 7, *A* and *B*). In contrast, intracellular administration of Ht31 into the postsynaptic neuron completely blocked LTD (Fig. 7, *A* and *B*). Surprisingly, Ht31 did not appear to affect basal transmission in these experiments as had previously been reported (Fig. 7*B*) (18, 19). We reasoned that the rundown of EPSCs might occur too rapidly to be detected due to the abrupt dialysis of the internal solution into the cell. Therefore, we repeated the experiment using recording pipettes with a higher series resistance (smaller tip diameter) to slow the rate of Ht31 diffusion into the neuron. This manipulation revealed the expected rundown of EPSCs as well as the occlusion of LTD (Fig. 7*C*). A repeated measure, ANOVA, confirmed a significant difference of EPSC amplitude with respect to time (Fig. 7*C*; $p < 0.05$). Post-hoc analyses revealed that the EPSCs within the first 6 min were statistically different from the rest of the base-line responses ($p < 0.05$). These results confirm the hypothesis that tonic phosphorylation of postsynaptic PKA substrates is critical for maintaining basal transmission in hippocampal slices and that dislodging PKA from AKAPs causes a rundown of excitatory transmission that occludes LTD.

DISCUSSION

Numerous studies of cultured hippocampal and cortical neurons have found that brief NMDA treatment stimulates a loss of surface expressed AMPA receptors, a phenomenon that is believed to provide a model for the study of LTD in the intact forebrain (34). We confirm and extend these findings by showing that a threshold level of NMDA receptor activation is required in hippocampal cultures to produce a stable change in AMPA receptor surface expression. Previous studies have also established that LTD at synapses in hippocampal area CA1 and the cerebral cortex is accompanied by dephosphorylation of postsynaptic PKA substrates (for review see Refs. 5 and 35). Here we show in cultured cortical neurons that NMDA treatment stimulates a loss of PKA from a synaptic biochemical fraction and that inhibiting PKA activity or disrupting PKA anchoring to AKAP is sufficient to reduce AMPA receptor surface expression in cultured hippocampal neurons. We further find in hippocampal slices that disruption of PKA-AKAP interactions causes a rapid rundown of AMPA receptor-mediated synaptic transmission that occludes the LTD that is induced by synaptic activation of NMDA receptors.

Our study has employed a number of preparations: low density hippocampal cultures for immunocytochemistry; high density hippocampal cultures for surface biotinylation; high density cortical cultures for biochemical fractionation; and intact hippocampal slices for electrophysiology. In doing so, we have followed a precedent set in a number of previous studies aimed at understanding LTD (for review see Refs. 10 and 36–38). While an internally consistent picture emerges from our results, it is important to recognize that these preparations may not always be directly comparable. Hippocampal neurons maturing under culture conditions may behave differently than neurons in an acutely prepared hippocampal slice. Moreover, although some forms of hippocampal and cortical LTD appear to be mechanistically identical, it is possible that the diversity of plasticity mechanisms at glutamatergic synapses parallels the diversity of neuronal types in both structures (39).

These caveats notwithstanding, our data suggest a hypothesis that appropriate activation of NMDA receptors may displace PKA from some synapses, thereby causing dephosphorylation of postsynaptic PKA substrates including AMPA receptors and depression of AMPA receptor-mediated transmission. Displacement of PKA from synapses in NMDA-treated cultures could account for the only partial recovery of AMPA receptor surface expression following treatment with PKA activators. This hypothesis is supported by the finding that activation of NMDA receptors on hippocampal neurons can also lead to a redistribution of the AKAP79/150-PKA complex away from synaptic sites (21). Ultimately, however, testing this hy-

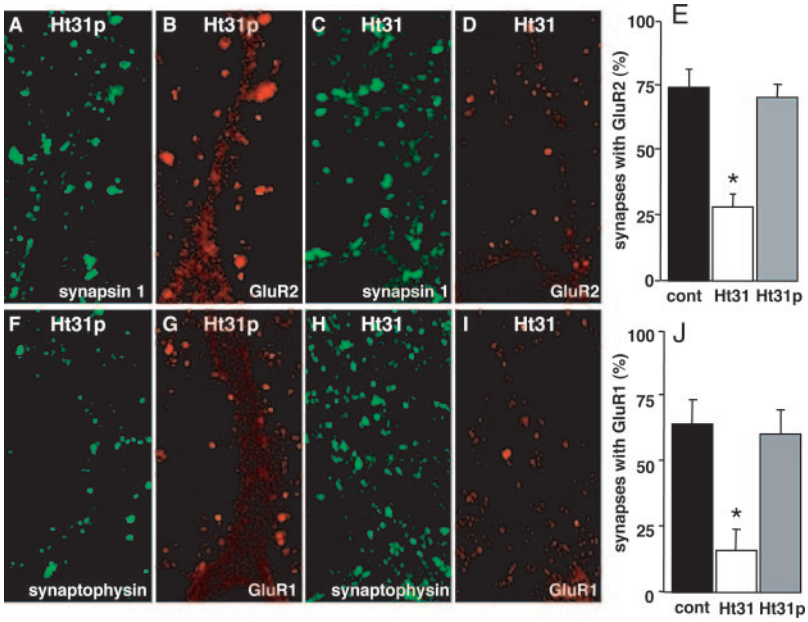

FIG. 6. **Disruption of PKA anchoring reduces synaptic AMPA receptors.** Cultures were treated with Ht31 or control Ht31p peptides and stained with antibodies against synapsin 1 (*A–D*) or synaptophysin (*F–I*) to mark synapses along with antibodies to the AMPA receptor subunit GluR2 (*A–D*) or GluR1 (*F–I*). In cultures treated with the control peptide Ht31p, synapsin and GluR2 staining overlapped frequently (*A* and *B*). Similarly, synaptophysin and GluR1 staining overlapped following Ht31p treatment (*F* and *G*). In contrast, in Ht31-treated cultures, staining for synaptic GluR2 was dramatically reduced (*C* and *D*). Ht31 similarly reduced staining for synaptic GluR1 (*H* and *I*). *E*, quantification of 150 synapses in 7 cells revealed that, in control-untreated cultures, 74 ± 8% synapsin puncta colocalized with GluR2. One hour following Ht31 treatment, 28 ± 6% synapsin puncta were associated with GluR2 staining (*, $p < 0.01$, *versus* control, Student's *t* test). Neurons treated with Ht31p exhibited GluR2 staining at 70 ± 6% synapses. *J*, quantification of synaptophysin and GluR1 staining revealed that, in control cultures, 64 ± 10% synapses were associated with GluR1, whereas Ht31 treatment reduced GluR1 staining to 15 ± 9% synapses (*, $p < 0.01$ *versus* control, Student's *t* test). In neurons treated with Ht31p, GluR1 was present at 60 ± 10% synapses.

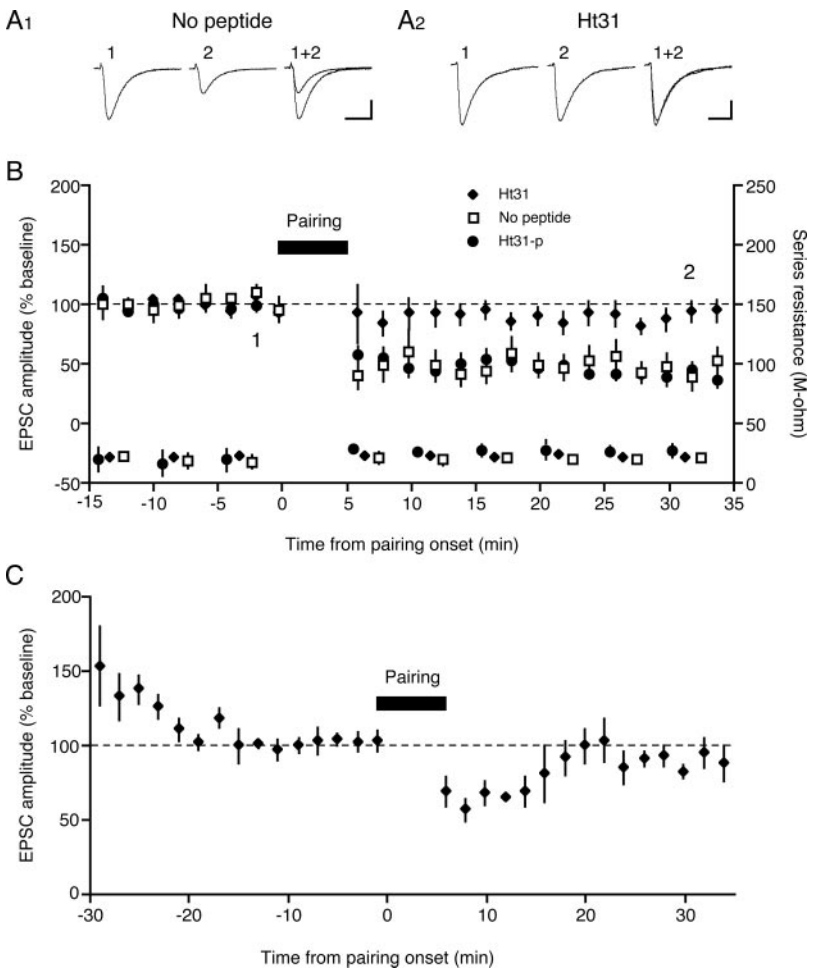

FIG. 7. **Ht31 produces EPSC rundown that occludes pairing-induced LTD in hippocampal slices.** *A*, sample sweeps before (*1*) and after (*2*) pairing-induced LTD under control conditions and during intracellular introduction of Ht31. Sweeps are the average of consecutive responses taken 5 min prior to pairing onset and 25–30 min following completion of the pairing protocol. For clarity, stimulus artifacts were blanked. Scale bars: 25 pA and 25 ms. *B*, overlay of grouped data time courses demonstrating blockade of LTD by Ht31. No peptide ($n = 5$) and Ht31p ($n = 5$) conditions manifested LTD, whereas ($n = 8$) prevented LTD. Each point represents data averaged into 2-min bins. Plotted on the leftward *y* axis is EPSC amplitude normalized to a 15-min base-line period. Plotted at the bottom of the graph are series resistance points that refer to the rightward *y* axis. The *black bar* indicates the duration of pairing of a 1-Hz stimulation with −40-mV membrane depolarization. *C*, experiments with a higher resistance pipette tip revealed a rundown of EPSCs that was not detected with larger tip pipettes (*B*). However, in both cases, the effect of Ht31 on LTD was the same.

pothesis will require high resolution molecular imaging and electrophysiology of individual synapses.

Our data are consistent with the hypothesis that dephosphorylation of PKA-AKAP substrates may initiate endocytosis of AMPA receptors. An alternative and not mutually exclusive possibility is that PKA activity may be required for constitutive exocytosis of AMPA receptors to the membrane. In the latter case, PKA inhibition could reduce surface expression of AMPA receptors by preventing delivery of new receptors to the membrane and the replacement of constitutively endocytosed synaptic receptors. Our data do not distinguish between these possibilities. However, disruption of PKA-AKAP anchoring with Ht31 causes a remarkably rapid rundown of synaptic transmission (>30% depression in <10 min; Fig. 7). Accounting for this change solely by blocking constitutive exocytosis would require a rate of AMPA receptor cycling that is far greater than what has been estimated in previous studies (10, 40, 41). Therefore, we favor the hypothesis that dephosphorylation of postsynaptic PKA substrates is a trigger for AMPA receptor endocytosis.

The finding that postsynaptic Ht31 mimics and occludes LTD in hippocampal slices implies that AKAP79/150 plays a key role in synaptic plasticity. Interestingly, AKAP79/150 levels increase during a late phase of long term potentiation (42). An intriguing possibility is that during LTD, the loss of the AKAP79/150-PKA complex from synapses (21) leads to decreases in levels of surface AMPA receptors, while during LTP, increased expression of AKAP79/150 may lead to increased insertion of synaptic AMPA receptors. Of course, because Ht31 globally disrupts PKA anchoring, further experiments are necessary to define a specific role for AKAP79/150 in these phenomena.

Finally, AKAP-mediated localization of PKA signaling may have important behavioral consequences. In Aplysia, Ht31-mediated disruption of binding of PKA to AKAPs blocks both short and long term facilitation. Interestingly, PKA regulatory subunit II levels at the synapse were also shown to increase during long term facilitation (43). Together with our work, these data suggest that altering the synaptic location of PKA may be a general mechanism to control substrate phosphorylation during synaptic plasticity. In addition, recent work indicates that disruption of PKA anchoring in the amygdala in mammals by injection of Ht31 blocks the naturally occurring plasticity required for auditory fear memory (44). Our data suggest that hippocampal-dependent memories may be similarly sensitive to disruption of PKA-AKAP interactions. Thus, modulation of PKA anchoring may have profound implications for physiology and behavior.

Acknowledgments—We thank B. Yoon, E. Sklar, and S. Meagher for assistance.

REFERENCES

1. Dudek, S. M., and Bear, M. F. (1992) *Proc. Natl. Acad. Sci. U. S. A.* **89,** 4363–4367
2. Kandler, K., Katz, L. C., and Kauer, J. A. (1998) *Nat. Neurosci.* **1,** 119–123
3. Kameyama, K., Lee, H. K., Bear, M. F., and Huganir, R. L. (1998) *Neuron* **21,** 1163–1175
4. Lee, H. K., Barbarosie, M., Kameyama, K., Bear, M. F., and Huganir, R. L. (2000) *Nature* **405,** 955–959
5. Lee, H. K., Kameyama, K., Huganir, R. L., and Bear, M. F. (1998) *Neuron* **21,** 1151–1162
6. Roche, K. W., O'Brien, R. J., Mammen, A. L., Bernhardt, J., and Huganir, R. L. (1996) *Neuron* **16,** 1179–1188
7. Banke, T. G., Bowie, D., Lee, H. K., Huganir, R. L., Schousboe, A., and Traynelis, S. F. (2000) *J. Neurosci.* **20,** 89–102
8. Beattie, E. C., Carroll, R. C., Yu, X., Morishita, W., Yasuda, H., von Zastrow, M., and Malenka, R. C. (2000) *Nat. Neurosci.* **3,** 1291–1300
9. Carroll, R. C., Lissin, D. V., von Zastrow, M., Nicoll, R. A., and Malenka, R. C. (1999) *Nat. Neurosci.* **2,** 454–460
10. Ehlers, M. D. (2000) *Neuron* **28,** 511–525
11. Man, Y. H., Lin, J. W., Ju, W. H., Ahmadian, G., Liu, L., Becker, L. E., Sheng, M., and Wang, Y. T. (2000) *Neuron* **25,** 649–662
12. Esteban, J. A., Shi, S.-H., Wilson, C., Nuriya, M., Huganir, R. L., and Malinow, R. (2003) *Nat. Neurosci.* **6,** 136–143
13. Lee, H. K., Takamiya, K., Han, J. S., Man, H., Kim, C. H., Rumbaugh, G., Yu, S., Ding, L., He, C., Petralia, R. S., Wenthold, R. J., Gallagher, M., and Huganir, R. L. (2003) *Cell* **112,** 631–643
14. Colledge, M., and Scott, J. D. (1999) *Trends Cell Biol.* **9,** 216–221
15. Bauman, A. L., and Scott, J. D. (2002) *Nat Cell Biol.* **4,** E203–E206
16. Carr, D. W., Stofko-Hahn, R. E., Fraser, I. D., Cone, R. D., and Scott, J. D. (1992) *J. Biol. Chem.* **267,** 16816–16823
17. Colledge, M., Dean, R. A., Scott, G. K., Langeberg, L. K., Huganir, R. L., and Scott, J. D. (2000) *Neuron* **27,** 107–119
18. Rosenmund, C., Carr, D. W., Bergeson, S. E., Nilaver, G., Scott, J. D., and Westbrook, G. L. (1994) *Nature* **368,** 853–856
19. Tavalin, S. J., Colledge, M., Hell, J. W., Langeberg, L. K., Huganir, R. L., and Scott, J. D. (2002) *J. Neurosci.* **22,** 3044–3051
20. Oliveria, S. F., Gomez, L. L., and Dell'Acqua, M. L. (2003) *J. Cell Biol.* **160,** 101–112
21. Gomez, L. L., Alam, S., Smith, K. E., Horne, E., and Dell'Acqua, M. L. (2002) *J. Neurosci.* **22,** 7027–7044
22. Snyder, E. M., Philpot, B. D., Huber, K. M., Dong, X., Fallon, J. R., and Bear, M. F. (2001) *Nat. Neurosci.* **4,** 1079–1085
23. Selig, D. K., Hjelmstad, G. O., Herron, C., Nicoll, R. A., and Malenka, R. C. (1995) *Neuron* **15,** 417–426
24. Chung, H. J., Xia, J., Scannevin, R. H., Zhang, X., and Huganir, R. L. (2000) *J. Neurosci.* **20,** 7258–7267
25. Harrison, D. A., Carr, D. W., and Meizel, S. (2000) *Biol. Reprod.* **62,** 811–820
26. Coghlan, W. M., Perrino, B. A., Howard, M., Langberg, L. K., Hicks, J. B., Gallatin, W. M., and Scott, J. D. (1995) *Science* **267,** 108–111
27. Klauck, T. M., Faux, M. C., Labudda, K., Langeberg, L. K., Jaken, S., and Scott, J. D. (1996) *Science* **271,** 1589–1592
28. Becker, J. W., Rotonda, J., Cryan, J. G., Martin, M., Parsons, W. H., Sinclair, P. J., Wiederrecht, G., and Wong, F. (1999) *J. Med. Chem.* **42,** 2798–2804
29. Bernstein, M. A., and Welch, S. P. (1998) *Eur. J. Pharmacol.* **341,** 173–177
30. Lee, H. W., Hahm, S. H., Hsu, C. M., and Eiden, L. E. (1999) *J. Neurochem.* **73,** 1769–1772
31. Liao, D., Hessler, N. A., and Malinow, R. (1995) *Nature* **375,** 400–404
32. Liao, D., Zhang, X., O'Brien, R., Ehlers, R. O., and Huganir, R. L. (1999) *Nat. Neurosci.* **2,** 37–43
33. Heynen, A. J., Quinlan, E. M., Bae, D. C., and Bear, M. F. (2000) *Neuron* **28,** 527–536
34. Malinow, R., and Malenka, R. C. (2002) *Annu. Rev. Neurosci.* **25,** 103–126
35. Heynen, A. J., Yoon, B. J., Liu, C. H., Chung, H. J., Huganir, R. L., and Bear, M. F. (2003) *Nat. Neurosci.* **6,** 854–862
36. Blanpied, T. A., Scott, D. B., and Ehlers, M. D. (2002) *Neuron* **36,** 435–449
37. Liao, D., Scannevin, R. H., and Huganir, R. (2001) *J. Neurosci.* **21,** 6008–6017
38. Kolleker, A., Zhu, J. J., Schupp, B. J., Qin, Y., Mack, V., Borchardt, T., Kohr, G., Malinow, R., Seeburg, P. H., and Osten, P. (2003) *Neuron* **40,** 1199–1212
39. Malenka, R. C., and Bear, M. F. (2004) *Neuron* **44,** 5–21
40. Lüscher, C., Xia, H., Beattie, E. C., Carroll, R. C., von Zastrow, M., Malenka, R. C., and Nicoll, R. A. (1999) *Neuron* **24,** 649–658
41. Passafaro, M., Piech, V., and Sheng, M. (2001) *Nat. Neurosci.* **4,** 917–926
42. Genin, A., French, P., Doyere, V., Davis, S., Errington, M. L., Maroun, M., Stean, T., Truchet, B., Webber, M., Willis, T., Richter-Levin, G., Sanger, G., Hunt, S. P., Mallet, J., Laroche, S., Bliss, T. V., and O'Connor, V. (2003) *Eur. J. Neurosci.* **17,** 331–340
43. Liu, J., Hu, J. Y., Schacher, S., and Schwartz, J. H. (2004) *J. Neurosci.* **24,** 2465–2474
44. Moita, M. A. P., Lamprecht, R., Nader, K., and LeDoux, J. E. (2002) *Nat. Neurosci.* **5,** 837–838